



On the strength of interplate coupling and the rate of back arc convergence in the central Andes: An analysis of the interseismic velocity field

Michael Bevis and Eric Kendrick

School of Ocean and Earth Science and Technology, University of Hawaii, 1680 East West Road, Honolulu, Hawaii 96822, USA (bevis@soest.hawaii.edu)

Robert Smalley Jr.

Center for Earthquake Research and Information, University of Memphis, 3890 Central Avenue, Suite 1, Memphis, Tennessee 38152, USA (smalley@ceri.memphis.edu)

Benjamin Brooks

School of Ocean and Earth Science and Technology, University of Hawaii, 1680 East West Road, Honolulu, Hawaii 96822, USA (bbrooks@soest.hawaii.edu)

Richard Allmendinger and Bryan Isacks

Department of Earth and Atmospheric Sciences, Cornell University, Snee Hall, Ithaca, New York 14853, USA (rwal@cornell.edu)

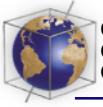
[1] **Abstract:** We interpret the interseismic crustal velocity field of the central Andes using a simple three-plate model in which the Andean mountain belt is treated as a rigid microplate located between the Nazca and South American (SoAm) plates. We assume that the Euler vectors associated with these plates are strictly coaxial and that the surface velocity field can be decomposed into an elastic loading field (driven by locking of the main plate boundary) and a smaller contribution associated with back arc convergence. We obtain our best fit to the geodetic velocities if the main plate boundary is fully (100%) locked between depths of ~10–50 km and ~8.5% of Nazca-SoAm plate convergence is achieved in the back arc (by underthrusting of the Brazilian Shield beneath the Subandean zone).

Keywords: Interseismic; velocity; elastic; deformation; central Andes.

Index terms: Continental contractional orogenic belts; crustal movements—intraplate; South America.

Received 28 June 2001; **Revised** 6 September 2001; **Accepted** 28 September 2001; **Published** 1 November 2001.

Bevis, M., E. Kendrick, R. Smalley Jr, B. A. Brooks, R. W. Allmendinger, B. L. Isacks, On the strength of interplate coupling and the rate of back arc convergence in the central Andes: An analysis of the interseismic velocity field, *Geochem. Geophys. Geosyst.*, 2, 10.129/2001GC000198, 2001.



the tectonics lies naked on the physical chart

S. Warren Carey

1. Introduction

[2] The central Andes incorporate two of the most striking features in the entire Andean mountain belt: the $\sim 55^\circ$ bend known as the Bolivian Orocline, and the Altiplano-Puna physiographic province, a high continental plateau second only to the Tibetan plateau in its area and average elevation [Allmendinger *et al.*, 1997]. Gephart [1994] pointed out the remarkable bilateral symmetry of central Andean topography and noted a less perfect but still rather striking mirror symmetry, relative to the same plane, in the morphology of the subducted Nazca slab (Figure 1). Paleomagnetic studies indicate rotation of the forearc and the mountain belt relative to the craton, with anticlockwise rotation dominating in the northern limb of the orocline and clockwise rotation in its southern limb [Isacks, 1988; Randall, 1998; Beck, 1998; Kley, 1999]. Isacks [1988] suggested that this pattern of rotation manifests along-strike variation in the magnitude of Neogene crustal shortening across the central Andes. Almost all of this shortening has taken place in the back arc region to the east of the Altiplano, consisting (from west to east) of the high Eastern Cordillera, the Interandean zone, and the low Subandean zone. (Note that some authors refer to the Interandean and Subandean zones jointly as the Subandean zone.) The youngest of these morphotectonic units, the Subandean zone, is a thin-skinned fold-and-thrust belt that has overthrust and is still overthrusting a slightly deformed foreland basin [Lamb, 2000]. According to Kley and Monaldi [1998] and Kley [1999], the degree of shortening within the Subandean zone, and within the broader back arc region, has a maximum value near the Santa Cruz elbow (and Gephart's plane of symmetry) and decreases fairly steadily both to the south and to the northwest. South of the Santa CruzM elbow, the Suban-

dean zone is believed to have formed after ~ 10 Ma [Gubbels *et al.*, 1993]. Given ~ 80 – 140 km of shortening within the Subandean zone (Table 1), achieved in ≤ 10 Myr, the implied average rate of shortening is ≥ 8 – 14 mm/yr.

[3] The direction of Nazca-South America (SoAm) convergence has changed very little in the last 20 Myr [Pardo-Casas and Molnar, 1987; Somoza, 1998]. While the rate of convergence has changed during this time period [Pardo-Casas and Molnar, 1987; Somoza, 1998; Norabuena *et al.*, 1999], at any given time the maximum rate of plate convergence along the entire plate boundary has consistently occurred in the central Andes. However, it is also true that, during this time period, the rate of Nazca-SoAm plate convergence has varied only slightly (in space) within the central Andean segment of the plate boundary. So what localized the lateral collapse of the central Andes and the associated growth of the Altiplano-Puna plateau? Isacks [1988] suggested that the bending and uplift of the central Andes was controlled by the geometry of the subducting Nazca plate (Figure 1). North and south of the central Andes the subducted slab lies very close to the bottom of the South American lithosphere, whereas beneath the central Andes the slab dips more steeply, and there is an asthenospheric wedge between the slab and the upper plate. This wedge both weakened the overlying lithosphere and accommodated (by flow) the downdip extension of the Brazilian Shield underthrusting the Andes in the back arc region. Wdowinski *et al.* [1989] invoked an additional role for slab geometry: the steepening of the slab beneath the central Andes promotes a flow field in the overlying mantle that exerts shear stresses on the base of the upper plate, dragging it into the slab and thereby throwing the leading edge of the SoAm plate into lateral compression. The morphology of the subducted slab also exerts a

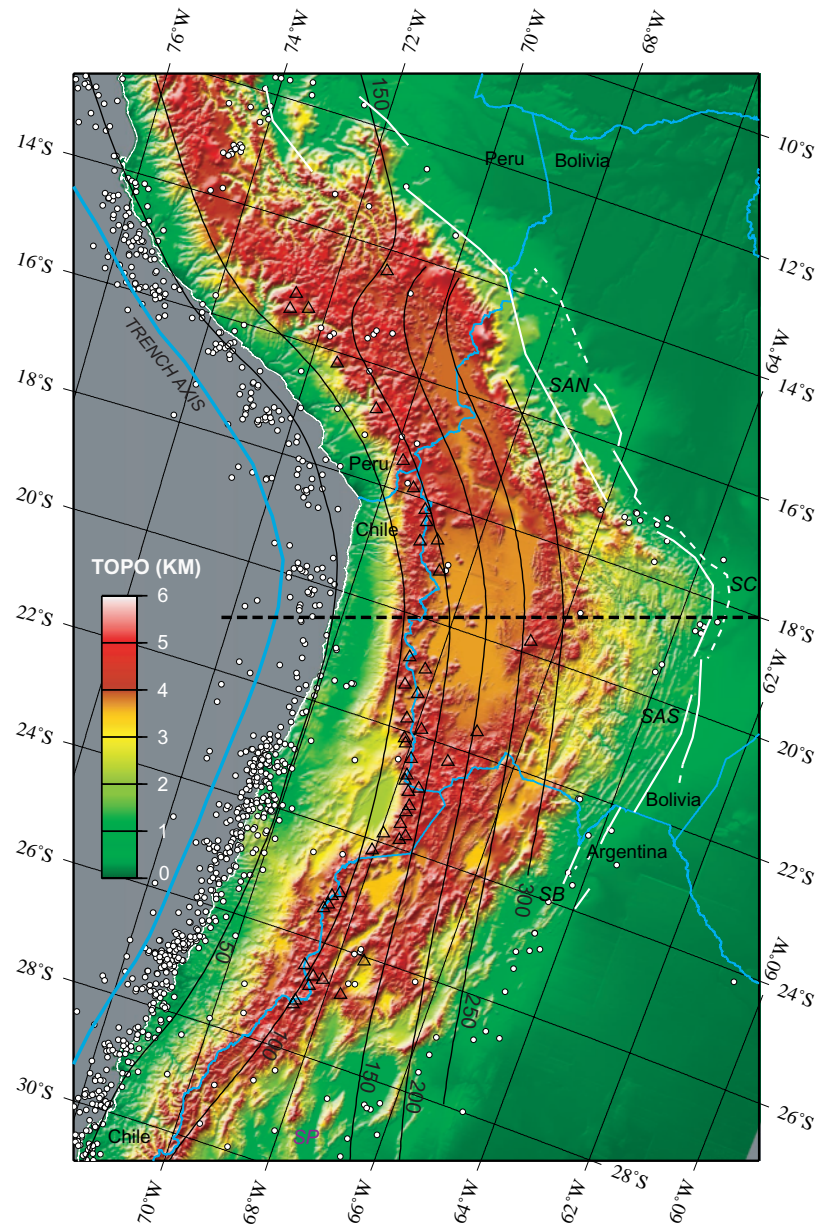
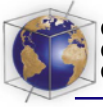


Figure 1. Topography and tectonic setting of the central Andes, presented in an oblique Mercator projection in which the “equator” is *Gephart’s* [1994] plane of symmetry (thick dashed black line). The light blue curve west of the coast is the trench axis. The black curves are the *Cahill and Isacks* [1992] depth contours (in kilometers) for the middle of the Wadati-Benioff zone. Note the “flat slab” sections of the subducted Nazca plate at the northern and southern limits of the map and the relatively steep slab underlying the central Andes. The white circles show all well-located shallow seismicity (1964–1995) from the catalog of *Engdahl et al.* [1998]. The open triangles indicate the active volcanic arc, which is limited to the steep slab segment. The outermost thrusts of the back arc (foreland) region, shown in solid white lines, indicate thrust faults which break the surface, whereas dashed curves indicate buried (blind) thrusts, some of which are inferred rather than observed. Abbreviations used in the figure: SAN, the northern Subandean zone; SAS, the southern Subandean zone; SC, Santa Cruz elbow; SB, Santa Barbara belt; SP, Sierras Pampeanas.

Table 1. Published Estimates of Horizontal Shortening in the Foreland Thrust Belt, Based on Balanced Cross-Section Analyses

Location	Shortening, km		Reference
	Subandean	Subandean and Interandean	
North Bolivia (14°–16°S)	74		<i>Baby et al.</i> [1996]
North Bolivia (14°–16°S)	135		<i>Baby et al.</i> [1995]
North Bolivia (14°–16°S)	132	156	<i>Roeder and Chamberlain</i> [1995]
South Bolivia (20°S)	100	159	<i>Dunn et al.</i> [1995]
South Bolivia (21°–22°S)		140–150	<i>Kley</i> [1993], <i>Kley et al.</i> [1996]
South Bolivia (21°–22°S)	86	125	<i>Baby et al.</i> [1997]
North Argentina (22°S)	60	75	<i>Mingramm</i> [1979], <i>Allmendinger et al.</i> [1983], <i>Allmendinger and Zapata</i> [2000]

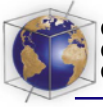
strong influence on the geometry of the active volcanic arc (Figure 1), as it does in other subduction zones [*Barazangi and Isacks*, 1977; *Bevis and Isacks*, 1984].

[4] Although the style of back arc shortening changes along the strike of the orogen [*Jordan et al.*, 1983], back arc shortening of one kind or another is characteristic of the Andes as a whole. The notion that the modern Andes, in general, were produced by lateral compression of the leading edge of the South American plate owing to the strong coupling of these plates at their interface [*Dewey and Bird*, 1970; *Uyeda*, 1982] draws support from the highly seismogenic character of this plate boundary. Chile alone suffers a magnitude 8 earthquake about once every 10 years. The recurrence interval for great earthquakes along most of the Nazca-SoAm plate boundary is of the order of 100 years. The central and southern Andes have the highest ratios of seismic to plate tectonic (or geodetic) slip of any subduction zone on Earth, and they are described as having very large coefficients of seismic coupling [*Ruff and Kanamori*, 1980; *Peterson and Seno*, 1984; *Kanamori*, 1986; *Scholz*, 1990]. The locking of the subduction interface during the interseismic phase of the earthquake cycle requires pervasive elastic straining of both plates. Because the locked plate interface has a shallow dip and dips down toward the upper plate,

interseismic straining at the Earth's surface is asymmetric: surface strain rates near the locked zone are much larger on the upper plate. Elastic loading signals of this kind have been measured by Japanese geodesists for more than 100 years. In the central Andes, direct geodetic observation of the earthquake deformation cycle began only during the last decade.

2. Crustal Velocity Field of the Central Andes

[5] The recent crustal velocity field of the central Andes, north of $\sim 23^\circ\text{S}$, is being measured by the South America-Nazca Plate Motion Project, known as SNAPP [*Norabuena et al.*, 1999] and by the central Andes GPS Project, known as CAP [*Kendrick et al.*, 1999; *Bevis et al.*, 1999]. *Kendrick et al.* [2001] analyzed all CAP and SNAPP data collected between January 1993 and March 2001 so as to produce an integrated velocity field for the central Andes. See *Kendrick et al.* [2001, Table 2] for a complete listing of station velocities expressed in a frame of reference attached to the stable core of the South American plate. The total observational time span varies greatly from one GPS station to another, from a minimum span of 2 years to a maximum span of more than 7 years. In this paper we make a preliminary analysis of this interseismic velocity field.



[6] Both the CAP and the SNAPP networks were constructed to study the interseismic, coseismic, and postseismic phases of the earthquake deformation cycle, as well as the neotectonic processes associated with mountain building. The biggest challenge presently facing crustal motion geodesists attempting to study the growth and development of mountain belts above strongly coupled subduction zones, such as the Andes, is isolating the displacements associated with orogenic processes from the much larger elastic signals, driven by locking of the main plate boundary, in which they are submerged. Given a hundred years or more of geodetic observations it would be easier to separate the transient horizontal and vertical signals associated with the earthquake deformation cycle from the permanent and progressive (i.e., nonreversing and accumulating) motions and deformations associated with intraplate deformation and the growth of topography. However, since the GPS networks of the central Andes are less than 10 years old, our sampling of the earthquake deformation cycle is highly incomplete. South of $\sim 23^{\circ}\text{S}$, the 1995 Antofagasta ($M_w = 8.0$) earthquake was observed by project CAP and, in considerably more detail, by our sister project SAGA [Klotz *et al.*, 1996, 1999]. In our present study area, north of 23°S , the only major earthquake to have occurred in the central Andes since geodetic measurements were initiated was the recent ($M_w = 8.4$) South Peru earthquake that occurred on 23 June 2001, just as the analysis for this paper was being completed. Accordingly, the velocity field analyzed here characterizes only the interseismic phase of strain accumulation preceding this great earthquake.

3. Modeling Elastic Strain in the Central Andes

[7] The sharp change in the trend of the central Andes, and the associated changes in the obliquity of plate convergence [McCaffrey, 1994],

should produce an unusual and characteristic signature in the elastic loading component of the velocity field. Bevis and Martel [2001] have used a simple, half-space elastic model to investigate interseismic strain accumulation above a subduction zone associated with oblique plate convergence. The horizontal surface velocity field near the leading edge of the upper plate is found to rotate as distance from the trench increases. Above the locked portion of the plate interface, surface velocity is more oblique than the plate convergence vector. Farther back, toward the interior of the upper plate, the surface velocity is less oblique than the plate convergence vector. This situation is illustrated in Figure 2a, in which the subduction zone has no map-view curvature and the obliquity of plate convergence does not change along strike. It is clear from Figure 2 that the surface velocity field associated with interseismic straining of the upper plate does not parallel the direction of plate convergence. Figures 2b and 2c depict bent plate boundaries characterized by two straight sections joined by a curved segment in which the locked plate interface has constant dip. Away from the bend, the interseismic velocity field rotates as in Figure 2a, emphasizing the strike-slip component of plate convergence above and just behind the locked zone and emphasizing the dip-slip component of plate convergence further back into the interior of the upper plate. Because the plate boundary is oceanward convex in Figure 2b but oceanward concave in Figure 2c, the directional fabric of the two velocity fields is quite different. Clearly Figure 2c is closer to the geometry we observe in the central Andes, though it differs from the real world example in several respects. Note that across the bend, the surface velocity field above the locked zone has a component of along-strike (or longitudinal) convergence and that the velocity field in the “northern” limb rotates counterclockwise (CCW), whereas the

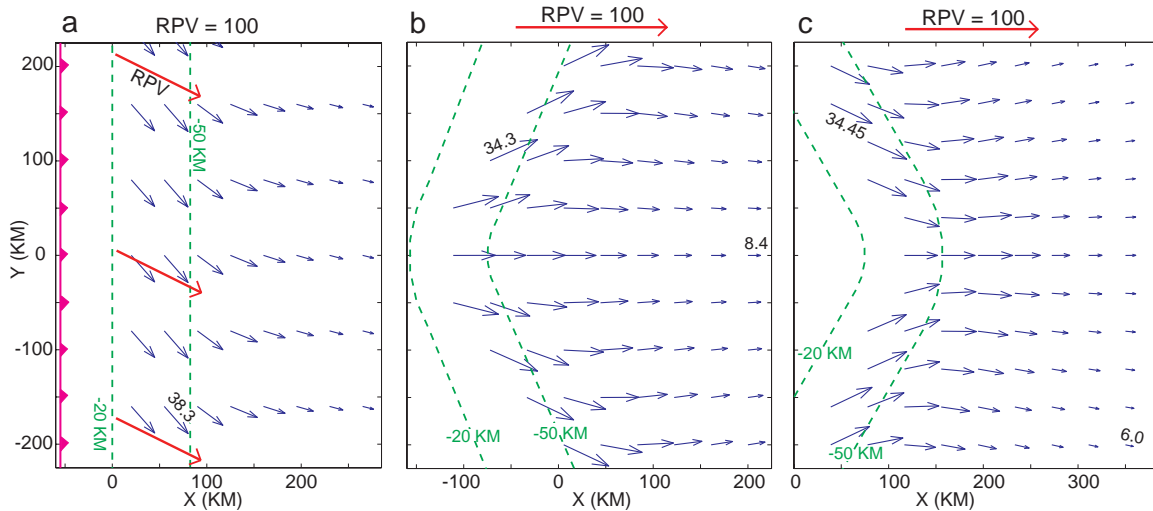
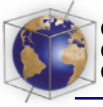


Figure 2. Synthetic examples of interseismic surface velocity fields produced by locking of plate boundaries associated with oblique plate convergence. In all three examples the locked plate interface dips at 20° between depths of 20 and 50 km, and its upper and lower edges are indicated using green dashed lines. The direction and magnitude of relative plate velocity are indicated using one or more thick red arrows, and the surface velocity field is depicted using a field of thin blue arrows. (a) The locked zone is straight in map view, and the relative plate velocity (RPV) has a uniform obliquity of 25° . (b) The locked zone is bent in map view. Two linear segments are joined by a curved segment with conical curvature. The obliquity of plate convergence varies between $+30^\circ$ and -30° and is zero at the center of the bend. (c) Shows a similar situation, but the map view curvature of the plate boundary has the opposite sense.

velocity field in the “southern” limb rotates in the opposite sense producing an along-strike divergence in the back arc (Figure 2c). This velocity field is reminiscent of one recently derived for the central Andes by *Lamb* [2000] using a fluid flow model in which buoyancy stresses play an important role. Indeed, the directional fabric of our Figure 2c and *Lamb*'s Figure 13a are strikingly similar. This similarity serves to remind us of the nonuniqueness problems inherent in any interpretation of crustal deformation data.

[8] We first attempt to model the GPS velocity field of the central Andes using a realistic geometrical model of the locked interplate boundary and a GPS-based Euler vector for Nazca-SoAm convergence but ignoring the role of back arc convergence. We assume that the interplate boundary is 100% locked in the

depth range 10–50 km (we considered scenarios with lower rates of locking, but they led to poorer fits with the GPS velocities). We estimated the geometry of the 50 km depth contour using the contour of *Cahill and Isacks* [1992] as a starting point and revised it using catalogs of earthquake hypocenters and centroid moment tensors (CMTs). We then determined a 10 km contour by interpolating between the 50 km contour and a three-dimensional space curve representing the depth at the axis of the Peru-Chile trench. We constructed a geometrical model for the locked zone by tiling the interval between the 10 and 50 km contours with a set of triangles (the green lines in Figure 3). We assumed an Euler vector (designated CAP05) whose components expressed in geocentric cartesian coordinates are $[\omega_x, \omega_y, \omega_z]' = [-0.191006, -4.66105, 8.78279]' \times 10^{-9}$ radians/yr (E. Kendrick et

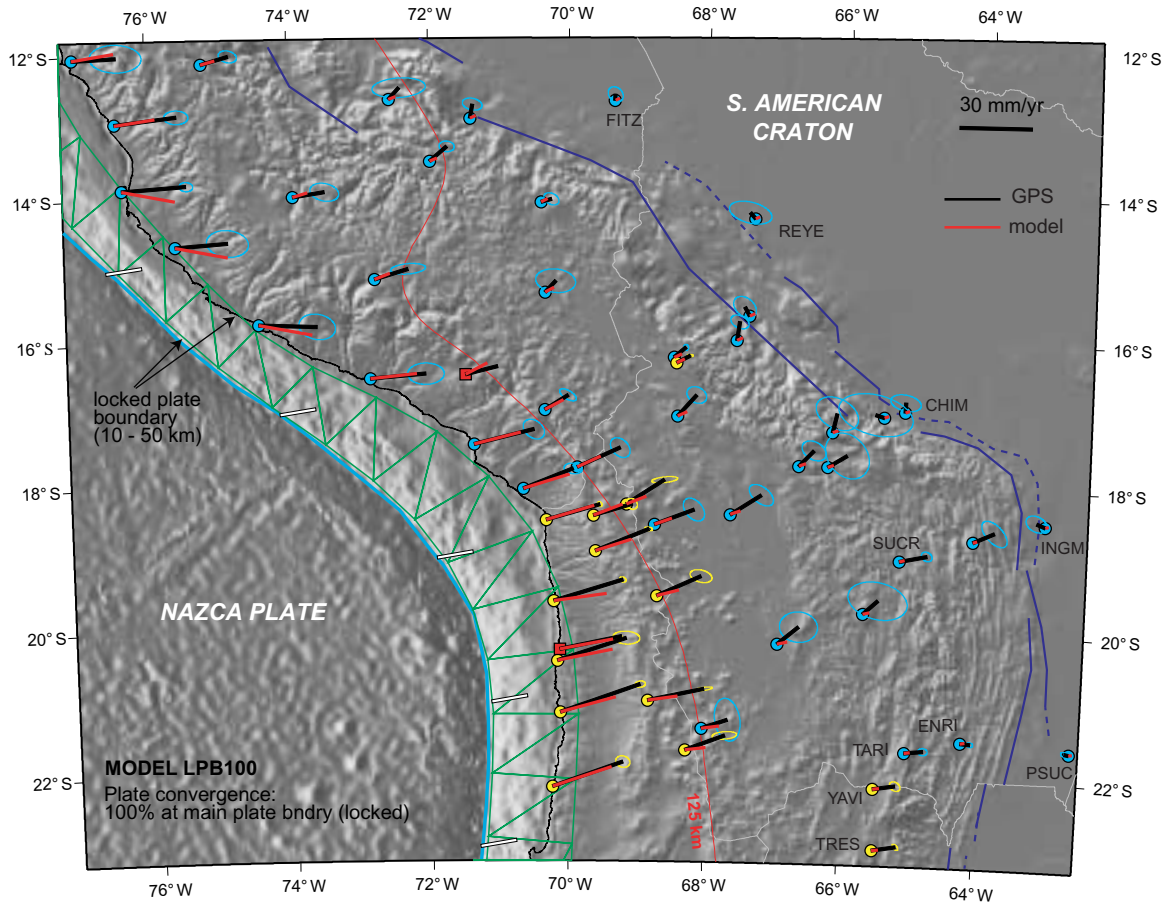
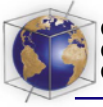


Figure 3. GPS velocities (black lines) compared with a model of the velocities (red lines) produced by elastic loading of the upper plate in response to locking of the main plate boundary (model LBP100). All velocities are relative to the effectively rigid core of the South American plate. Stations belonging to the SNAPP and CAP networks are colored blue and yellow, respectively. Some stations are labeled with their four letter station codes. The error ellipses are nominally 95% confidence ellipses. The white rectangles near the trench axis indicate the direction, but not the magnitude, of Nazca - South America plate convergence, as predicted by the Euler vector designated CAP05.

al., manuscript in preparation, 2001). This Euler vector predicts relative plate velocities (in the central Andes) very similar to those predicted by *Angermann et al.* [1999], except that our velocity vectors are rotated 3° – 4° clockwise relative to theirs. Between 13° and 30° S, the Nazca-SoAm convergence rates predicted by CAP05 (at the trench axis) fall in the range 61.5–63.4 mm/yr, with the maximum value occurring near 26° S.

[9] We model the elastic loading signal produced by locking of the plate boundary using the well-known backslip formalism of *Savage* [1983]. Like *Bevis and Martel* [2001] we implemented this computation in an elastic halfspace, but in this study we utilized triangular rather than rectangular dislocation elements, employing the equations provided by *Comninou and Dundurs* [1975] and the general approach of *Jeyakumaran et al.* [1992].

An oblique Mercator projection, designed to minimize the distortion of angles and lengths within the study area, was used to project all geometrical elements, including the triangular dislocation network and the Euler velocity field, into an elastic halfspace. For each triangular element, we computed the plate convergence vector at the centroid of the element (in geospace), transformed this vector into the halfspace, and projected it onto the surface of the dislocation, readjusting its length so as to maintain the magnitude of relative plate velocity, but reversing its sign, so to generate backslip. (To simulate partial locking of the plate boundary, we reduce the backslip velocity by multiplying it by the locking rate.) We computed the surface displacement at each GPS station for every triangular element in the dislocation network and computed the net motion by linear superposition. The observed and model velocity fields are compared in Figure 3. We call this model LPB100 because it invokes a locked plate boundary (LPB) and assumes that 100% of Nazca-SoAm plate convergence is achieved at this boundary.

[10] The elastic loading model, LPB100, predicts velocities (the red lines in Figure 3) that are in reasonable agreement with the GPS results near the coast but are much smaller than the GPS velocities for stations located in the eastern half of the mountain belt (particularly so near the Santa Cruz elbow). That is, the model velocity field decays much more rapidly with increasing distance from the coast than does the geodetic velocity field. Two possible explanations for this finding are fairly obvious. First we implemented the backslip model in an elastic halfspace, whereas at interseismic timescales, sub-lithospheric mantle acts as a fluid and not as an elastic solid. It would be better to implement the backslip model in an elastic plate rather than an elastic halfspace. This would cause the (elastic) surface velocity field

to decay more slowly (spatially) toward the interior of the upper plate. Second, our model completely neglected any crustal velocity component associated with back arc convergence. There is ample geological evidence for shortening of ≥ 8 mm/yr across the southern Subandean zone since 10 Ma (Table 1). At stations TRES, YAVI, TARI, and ENRI, where the measurement errors are relatively small, the elastic model seriously underpredicts the observed velocities. However, it is also clear that the GPS velocities are declining quite rapidly to the east as one approaches the outermost thrusts of the Subandean zone. (Note that station PSUC, in the craton, is essentially stationary.) The suggestion is that the observed velocities at these stations derive primarily from shortening within the Subandean zone rather than from elastic signals produced by locking of the main plate boundary. Accordingly, we leave consideration of plate rather than halfspace models of interseismic straining to a later work, and we focus in the rest of this paper on extending our existing velocity model by incorporating a contribution from back arc convergence.

4. Extending the Velocity Model to Incorporate Back Arc Convergence

[11] According to *Gubbels et al.* [1993], sometime after 10 Ma, the Eastern Cordillera began to overthrust the Brazilian shield on a midcrustal detachment that merges updip with the master décollement (basal detachment) of the Subandean zone. The Eastern Cordillera acted as a “bulldozer” that drove the development of the Subandean fold and thrust belt by shearing the Phanerozoic cover off the underthrusting Brazilian shield. The simplest way to explain both the geological observations and the GPS velocity gradient observed across the Subandean zone is to assume that the décollement underlying the Subandean zone is freely slipping at depth but locked near the front (i.e.,

eastern edge) of the fold-thrust belt. Since the décollement is both shallow and very gently dipping near the deformation front, the effects of locking would be highly localized in space: they would not extend very far west of the bottom of the locked zone. In order to model this process in any detail, we need to know the geometry of the locked portion of the décollement. This is not known a priori, and given the sparsity of the present GPS networks, it probably cannot be inverted from the GPS observations with any great confidence. However, since the influence of locking would be localized, we can infer the impact of back arc convergence on the velocity field well to the west of the locked portion of the décollement: it should be very similar to the influence of a freely slipping décollement. Accordingly, we next consider the velocity field associated with a locked main plate boundary and a freely slipping back arc décollement, and we defer consideration of back arc locking to a later section of this paper.

[12] The simplest way in which to implement a model with a locked plate boundary and a freely slipping back arc décollement is to construct a three-plate model in which the Andean mountain belt is treated as a rigid microplate located between the Nazca plate and the South American plate and to assume that the Euler vectors for Nazca-Andean motion and Andean-SoAm motion are coaxial. That is, the Nazca-SoAm convergence is partitioned between the Nazca-Andean boundary (i.e., what we have been calling the “main plate boundary,” which is partially or wholly locked) and the Andean-SoAm boundary (which we assume, for now, to be freely slipping). We explored the impact of various locking rates on the main plate boundary, as well as the ratio of forearc to back arc convergence. In Figure 4 we show our best fit model in which 91.5% of Nazca-SoAm convergence is assigned to the main

plate boundary, which is 100% locked at depths of 10–50 km, and the remaining 8.5% of plate convergence is assigned to a décollement that nominally daylight at the dashed magenta line. We call this model FSD8.5C, since it assumes that a freely slipping décollement (FSD) accounts for 8.5% of Nazca-SoAm convergence (8.5) and that the three Euler vectors associated with the three plates are strictly coaxial (C). As long as we ignore shallow locking of the décollement, the precise position of its surface trace is not important: all stations to the west of this trace get a velocity boost due to Andean-SoAm convergence, and all stations to the east of it do not. All we really need to know for now is which stations lie above or to the west of the décollement and which stations lie in the craton.

[13] The augmented model, FSD8.5C, produces a much better fit to the GPS velocities (Figure 4) than did the previous model, LPB100 (Figure 3). The residual velocity field, defined as the vector velocity difference (observed-model), is shown in Figure 5. In the eastern Andes the fit is good south of $\sim 18^\circ\text{S}$ and very good south of $\sim 20^\circ\text{S}$. The fit is also very good almost everywhere in Peru. The largest problems occur in the Chilean forearc and in the back arc of western Bolivia. The group “G1” of stations enclosed by the dashed magenta curve in Figure 5 has spatially coherent residuals, with magnitudes of 3–5 mm/yr, oriented roughly NE. A second group of stations, including LEON, CNOR, SAPE, TUNA, and CHIM, has residual velocities of similar or even greater magnitude, oriented W-NW, though some of these also have large error ellipses. Even though the disagreement between the GPS estimate and the model velocity is often not significant or is only marginally significant (statistically) at a given station, the fact that groups of stations have similar misfits

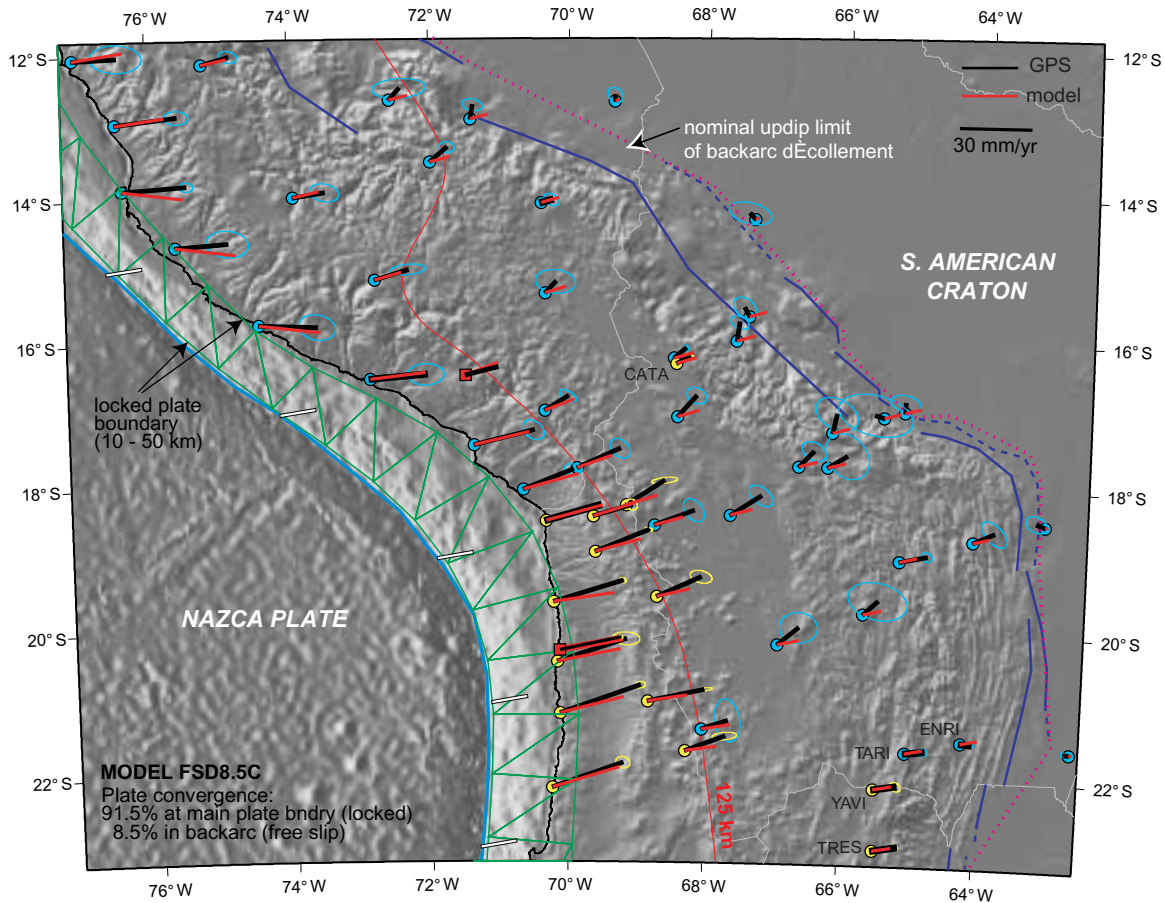
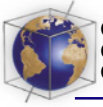


Figure 4. GPS velocities (black lines) compared with those predicted by the three-plate model FSD8.5C (red lines). Other symbols as in Figure 3.

suggests that model FSD8.5C has systematic problems in this part of the central Andes.

[14] Nearly all the SNAPP stations have a total observational time span of ~ 2.1 years, which is about the minimum useful time interval for velocity estimation (given just two GPS campaigns). Our experience in South America and elsewhere indicates that one must be careful not to overinterpret velocity estimates based on such a short time span. The fact that the CAP and SNAPP stations with the longest time spans tend to have smaller residuals than their sister stations reinforces the need for caution.

Nevertheless it is of some interest to consider how one might modify the model (FSD8.5C) to account for the apparent discrepancies between its predictions and the GPS measurements. If we were to assume that the décollement beneath the northern Subandean zone (SAN in Figure 5) was fully locked down to a depth contour located (in map view) near to or west of the Eastern Cordillera Frontal Thrust (ECFT in Figure 5), then the predicted back arc component of velocity at stations CHIM, TUNA, and SAPE would be greatly reduced, and these stations would be nearly stationary, in accord with the GPS measurements. Depending on the

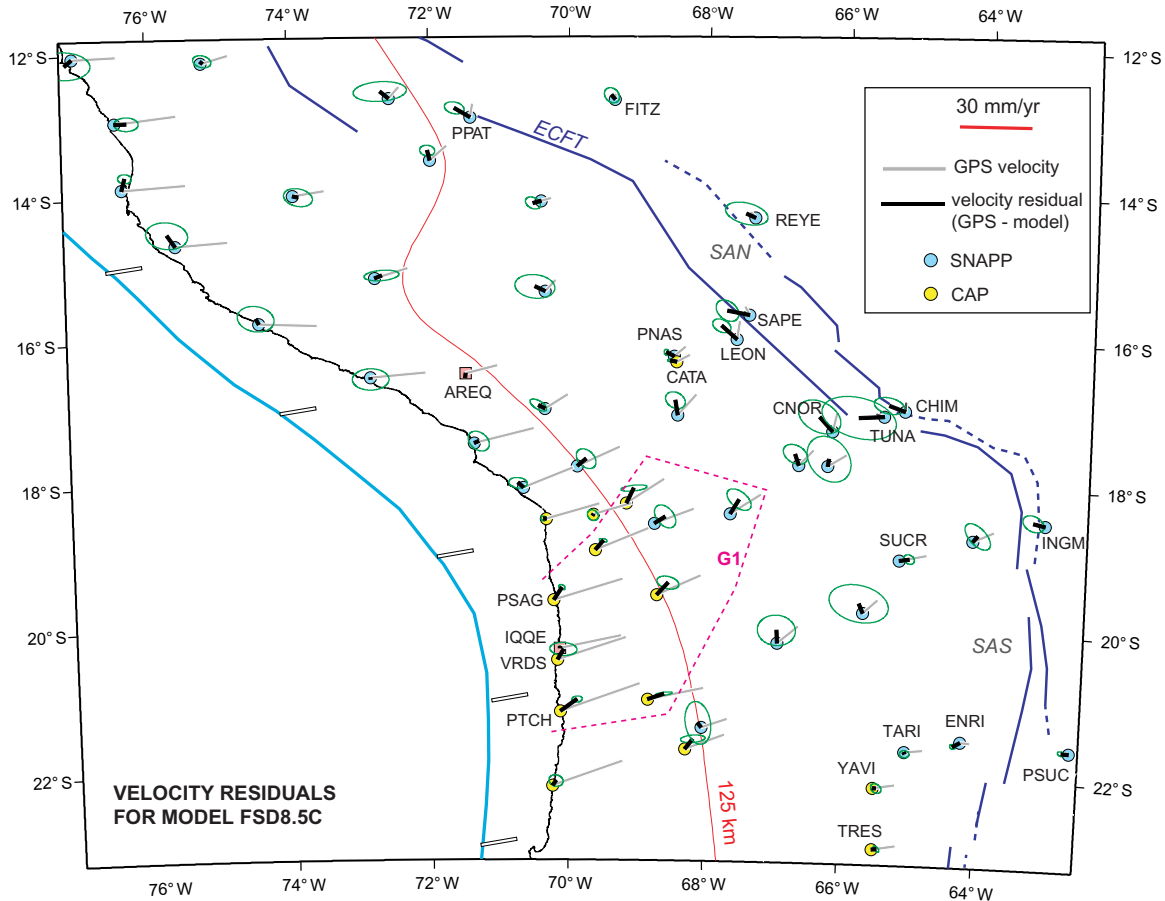
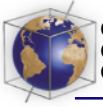
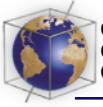


Figure 5. Velocity residuals (observed-calculated) for model FSD8.5C (thick black lines). The GPS velocities are also shown (subdued gray lines). The 95% error ellipses refer to the residuals rather than the observed GPS velocities, so to assist the reader in determining the significance of the misfit at each station. Note, for example, that while station TUNA has the biggest residual, it also has the largest uncertainty.

precise geometry of the lower portion of this locked zone, the residuals at LEON and CNOR could be reduced too, though it is hard to see how the north component of these velocity residuals could be eliminated.

[15] It is possible that our geometrical model for the locked plate boundary near station IQQE is inaccurate and, as a result, that we have underestimated the elastic loading signal at the stations in group G1. It would be helpful if the seismologists working on the interplate seismicity of the Andes could provide us with

better, and geometrically more explicit, models for the zone of shallow underthrusting. (Vertical sections depicting interplate seismicity would be more useful if they were always labeled with the latitudes and longitudes of both end points. It would be even more convenient if the interplate zone of seismicity were characterized as a surface in three-space, rather than as one or more curves presented graphically in vertical sections.) Additionally, we can probably improve our mathematical model for the deformation associated with locking of the main plate boundary by implementing our



elastic computations in an elastic plate rather than an elastic half-space.

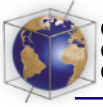
[16] We could obtain a better fit to our GPS results if we abandoned the three-plate model with its coaxial Euler vectors. If we assumed instead that the motions of the southern and northern limbs of the orocline (relative to the craton) could be described using different Euler vectors, we could certainly reduce many of the larger residuals that presently occur near the Iquique-Santa Cruz axis (Gephart's axis of symmetry), particularly if we allowed both north limb-craton and south limb-craton convergence to be modeled using poles that could differ from the pole of Nazca-SoAm convergence. However, this four-plate model would imply relative motion of the northern and southern limbs of the orocline near their junction, and there are no major transverse structures (cutting right across the orogen) nor lines of shallow seismicity to accommodate or manifest active tectonic segmentation of this kind. However, *Lamb* [2000] has argued rather convincingly that oroclinal bending is an ongoing tectonic process and that the strains associated with bending are accomplished diffusely by suites of relatively minor structures. We are reluctant to "escalate" our modeling in this way until another round of GPS measurements has been completed and analyzed and we can be sure that the residuals in Figure 5 do not derive from measurement errors. Nevertheless, such an escalation may eventually prove necessary. In the meantime our simple three-plate model can serve as a conceptual point of departure for researchers considering more complicated models.

5. Present Rate of Shortening in the Southern Subandean Zone

[17] The stations TRES, YAVI, TARI, ENRI, and PSUC, which span the southern Subandean

zone near the border between Bolivia and Argentina, have some of the best-constrained velocity solutions in the central Andes. The GPS velocity estimates for stations TRES, YAVI, and TARI have magnitudes of 8–10 mm/yr and are oriented very close to N82°E. The GPS velocity at ENRI is just 4.1 mm/yr, N94°E, while PSUC is nearly stationary. According to our simple half-space model, the elastic loading signal associated with locking of the main plate boundary is 2.6 mm/yr at YAVI and TRES, 2.3 mm/yr at TARI, and 1.9 mm/yr at ENRI. This component is a transient elastic signal that will be reversed during a future earthquake and therefore does not contribute to long-term geological change. By subtracting this elastic contribution from the average velocity of stations TRES, YAVI, and TARI, we find the net rate of shortening between these stations and the craton is ~6.5 mm/yr. (Because model FSD8.5C tries to fit the entire central Andes and not just the area near 22°S, it predicts only 5.4 mm/yr of back arc convergence in this part of the orogen.) We can explain the velocity at ENRI, which is only about half of the mean velocity of TRES, YAVI, and TARI, by supposing that shortening is still occurring in the Subandean (and Interandean) fold and thrust belt between TARI and ENRI. Alternatively, and perhaps more plausibly, we can assume that nearly all geological (long-term, progressive) shortening east of TARI occurs east of ENRI, near the front of the Subandean zone, but that the shallow part of its basal detachment is presently locked, and this is producing an elastic signal which decays rapidly to the west but is still strong enough at ENRI to suppress about half of the velocity associated with back arc convergence.

[18] There is some seismicity in the Subandean zone, but the rate of moment release is low compared to the "flat slab" regions north or south of the central Andes [*Jordan et al.*, 1983]. Figure 1 shows all well-located shallow

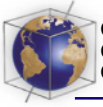


events in the time interval 1964–1995. Available focal mechanisms indicate less than a dozen or so earthquakes, all minor, that could plausibly manifest underthrusting on the master detachment underlying the Subandean zone and, given poor depth control, some of these could be located above or below the detachment and so represent activity on other faults [Jordan *et al.*, 1983; Chinn and Isacks, 1983; Cahill *et al.*, 1992; Lamb, 2000]. So the seismological evidence indicates that most of the detachment has been aseismic for ~ 40 years, and therefore it has been either freely slipping or continuously locked. The GPS velocity field suggests that lower portion of the detachment is freely slipping and the upper part is locked. Shallow locking of at least the updip edge of the basal detachment is expected in the southern Subandean zone, since the detachment does not actually reach the surface. We need a denser GPS network to better elucidate the pattern of shallow locking.

[19] Station SUCR, well to the north of TARI but in a similar tectonic setting, has a well-constrained velocity solution of ~ 11.6 mm/yr. The elastic contribution from the main plate boundary is only 2.1 mm/yr, implying that at 18° – 19° S the Subandean zone is shortening at ~ 9.5 mm/yr. This is considerably larger than the 6.5 mm/yr of shortening estimated farther south, near 22° S. However, both estimates are smaller than the rates suggested by balanced cross-section analysis of the fold and thrust belt (Table 1). Prior interpretations of a 10 Ma date for the initiation of thrusting in the Subandean belt were based on regional correlations of marine strata of that age (the “Yecua” formation). More recent geochronological work has suggested that the correlated strata are locally as old as 14 Ma and as young as 8 Ma with one questionable section yielding a much older age still. In other words, the previous correlations are probably incorrect. A more reliable, though indirect, estimate of the age of initiation of

Subandean/Interandean deformation can be made by determining the age that significant shortening ceased in the Eastern Cordillera. That age [Gubbels *et al.*, 1993] ranges from 9 to ~ 13 Ma. Given the uncertainties in the estimates of the magnitude of shortening along any particular section, combined with the lack of knowledge about exactly when Subandean deformation began, the geological data can be interpreted to be identical to the geodetic estimates for the rate of back arc deformation or could be 30–50% higher. Work currently in progress should improve this situation in the near future.

[20] If the present hint that the geological rates of shortening are higher than the geodetic rates is verified by future work, a possible explanation for this discrepancy is that the rate of shortening in the Subandean zone has been steadily decreasing during the time that this foreland belt has been forming. According to Somoza [1998] the Nazca-SoAm convergence rate at $\sim 22^\circ$ S has fallen by 5.7 mm/yr per Myr since ~ 10.8 Ma. This implies that the present convergence rate is only $\sim 69\%$ of the average rate for the last 10 Myr. Since plate convergence is the primary driver of back arc convergence, we might expect a similar difference between the geological estimates for shortening in the Subandean zone and the geodetic estimates for the present rate of back arc convergence. Assuming the Subandean zone formed nearly 10 Myr ago or more recently, its average rate of shortening has been at least 8–14 mm/yr, and applying a factor of 0.69 implies a present-day rate of at least 5.5–9.5 mm/yr, which compares reasonably well with the present GPS results. (However, this argument may be simplistic in that plate convergence may drive back arc shortening indirectly, via the growth of regional topography and the onset of gravitational spreading. In this case a slowing of plate convergence might not lead to an imme-



diate drop in the rate of back arc shortening driven by gravitational spreading.)

[21] The deformation front of the southern Subandean belt is commonly thought to be blind; that is, the décollement does not come up to the surface but dies out in a buried tip line. The fact that stations PSUC and INGM are not moving relative to the craton suggests that they are located east of the deformation front. The same is true of stations CHIM, REYE, and FITZ further north. The precise location of the deformation front is not yet known.

6. Conclusions

[22] Like *Norabuena et al.* [1998], we find it necessary to invoke both elastic loading (produced by locking of the main plate boundary) and back arc convergence (underthrusting of the Brazilian Shield) in order to explain the recent crustal velocity field of the central Andes. Largely because of a systematic difference between the velocity fields that *Norabuena et al.* [1998] and *Kendrick et al.* [2001] attained for Bolivia and Peru, our models differ in detail. We find no compelling evidence for slip partitioning on trench-parallel structures in the Peruvian forearc. Instead we prefer to explain the curvature of the forearc velocity field as a manifestation of elastic strain partitioning controlled by along-strike changes in the obliquity of plate convergence [*Bevis and Martel*, 2001]. *Norabuena et al.* [1998] concluded that the main plate boundary was only partially ($\sim 50\%$) locked, but we find it necessary to invoke 100% locking of this plate boundary. Small changes to the upper and lower locking depths (10 and 50 km) in our model have only a modest effect on the predicted velocity field, but changes in the locking rate produce directly proportional changes in the elastic component of velocity. Our finding of 100%, or nearly 100%, coupling across the main plate boundary is consistent with the

highly seismogenic character of this plate boundary. Our model requires that only $\sim 8.5\%$ of total Nazca-SoAm plate convergence (5–6 mm/yr) takes place in the back arc, which is significantly less than the 10–15 mm/yr estimated by *Norabuena et al.* [1998].

[23] The best-constrained GPS velocity estimates imply that the modern rate of shortening in the southern Subandean zone increases from ~ 6.5 mm/yr near 21.5°S to about 9.5 mm/yr near 18.5°S , implying that eastward motion of the forearc and central core of the mountain belt cannot be explained completely by a rigid body motion. The geologically determined shortening rates within the Subandean zone are less well constrained than the geodetic rates. Not only is it difficult to accurately determine total shortening using balanced cross sections, but the total time taken for the Subandean zone to form is not yet well constrained. Accordingly, it is probably premature to place any great significance on the apparent discrepancies between the geological and the geodetic rates. While the differences between the geodetic and geologic rates are probably not statistically significant, geological estimates of shortening rate allow (and perhaps suggest) that the rate of back arc shortening varies with latitude, and the GPS results seem to suggest the same thing. When projects SNAPP and CAP produce improved geodetic velocity estimates in the near future, it may be necessary to move beyond the simple three-plate model. However, significant densification of these GPS networks will be required (at least locally) to fully realize their potential impact on our understanding of the various tectonic and seismogenic processes currently operating in the central Andes.

[24] While the insights obtained by combining geodetic and geological studies of the central Andes are largely kinematical in nature, they should allow us to integrate our measurements

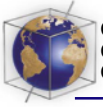
over a range of timescales and so provide much stronger constraints on geodynamical models of the mountain building process. The prospect of soon being able to separate the forearc-driven and back arc-driven components of the surface velocity and strain fields should also interest seismologists working on the earthquake deformation cycle.

Acknowledgments

[25] We dedicate this paper to Michael Mayhew and Dan Weill of the National Science Foundation on the occasion of D. Weill's recent retirement. From the mid 1980s to the early 1990s, Mayhew's program funded a large fraction of all GPS-based crustal motion research in the United States, often taking the unusual step of funding projects for 5 years, thereby allowing investigators the time they needed to develop the promise of GPS geodesy. If Mayhew helped nurture this revolutionary technique, D. Weill played a key role in its subsequent consolidation by overseeing many grants of GPS equipment to the geophysical community and by his long-term funding and fostering of the University NAVSTAR Consortium (UNAVCO). We thank our many coworkers in South America and Tim Dixon, Seth Stein, et al., of our sister project SNAPP, for their critical roles in the production of the velocity field interpreted in this paper. We thank Renata Dmowska and Goran Ekstrom for helpful discussions and Robert Reilinger and Simon Lamb for their very useful reviews of an earlier version of this paper. This research was supported by the National Science Foundation through grants EAR-9116733 and EAR-9596061. This is SOEST contribution 5836 and CERi contribution 436.

References

- Allmendinger, R. W., and T. R. Zapata, The footwall ramp of the Subandean decollement, northernmost Argentina, from extended correlation of seismic reflection data, *Tectonophysics*, 321, 37–55, 2000.
- Allmendinger, R. W., V. A. Ramos, T. E. Jordan, M. Palma, and B. L. Isacks, Paleogeography and Andean structural geometry, northwest Argentina, *Tectonics*, 2, 1–16, 1983.
- Allmendinger, R., T. Jordan, S. Kay, and B. Isacks, The evolution of the Altiplano-Puna Plateau of the Central Andes, *Ann. Rev. Earth Planet. Sci.*, 25, 139–174, 1997.
- Angermann, D., J. Klotz, and C. Reigber, Space-geodetic estimation of the Nazca-South America Euler Vector, *Earth Planet. Sci. Lett.*, 171, 329–334, 1999.
- Baby, P., I. Moretti, B. Guillier, R. Limachi, E. Mendez, J. Oller, and M. Specht, Petroleum system of the northern and central Bolivian Sub-Andean zone, in *Petroleum basins of South America: Amer. Assoc. Petrol. Geol. Mem.*, vol. 62, edited by A. J. Tankard, S. R. Suárez, and H. J. Welsink, pp. 445–458, Tulsa, Okl., 1995.
- Baby, P., P. Rochat, G. Hérail, G. Mascle, and A. Paul, Neogene thrust geometry and crustal balancing in the northern and southern branches of the Bolivian orocline (Central Andes), paper presented at 3rd International Symposium on Andean Geodynamics, St. Malo, France, 1996.
- Baby, P., P. Rochat, G. Mascle, and G. Hérail, Neogene shortening contribution to crustal thickening in the back arc of the Central Andes, *Geology*, 25, 883–886, 1997.
- Barazangi, M., and B. Isacks, Spatial distribution of earthquakes and subduction of the Nazca plate beneath South America, *Geology*, 4, 686–692, 1977.
- Beck, M., On the mechanism of crustal block rotations in the Central Andes, *Tectonophysics*, 299, 75–92, 1998.
- Bevis, M., and B. L. Isacks, Hypocentral trend surface analysis: Probing the geometry of Benioff zones, *J. Geophys. Res.*, 89, 6153–6170, 1984.
- Bevis, M., et al., Crustal motion north and south of the Arica deflection: Comparing recent geodetic results from the Central Andes, *Geochem. Geophys. Geosyst.*, 1, Paper 1999GC000011, 1999. (Available at <http://g-cubed.org>)
- Bevis, M., and S. Martel, Oblique plate convergence and interseismic strain accumulation, *Geochem. Geophys. Geosyst.*, 2, Paper number 2000GC000125, 2001. (Available at <http://g-cubed.org>)
- Cahill, T., and B. Isacks, Seismicity and shape of the subducted Nazca plate, *J. Geophys. Res.*, 97, 17,503–17,529, 1992.
- Cahill, T., B. Isacks, D. Whitman, J.-L. Chatelain, A. Perez, and J.-M. Chiu, Seismicity and tectonics in Jujuy Province, northwestern Argentina, *Tectonics*, 11, 944–959, 1992.
- Chinn, D., and B. Isacks, Accurate source depths and focal mechanisms of shallow earthquakes in western South America and in the New Hebrides Island Arc, *Tectonics*, 2, 529–563, 1983.
- Comninou, M., and J. Dundurs, The angular dislocation in a half-space, *J. Elasticity*, 5, 203–216, 1975.
- Dewey, J., and J. Bird, Mountain belts and the new global tectonics, *J. Geophys. Res.*, 75, 2625–2647, 1970.
- Dunn, J. F., K. G. Hartshorn, and P. W. Hartshorn, Structural styles and hydrocarbon potential of the Sub-An-



- dean thrust belt of southern Bolivia, in *Petroleum Basins of South America*, vol. 62, edited by A. J. Tankard, S. R. Suárez and H. J. Welsink, pp. 523–543, Am. Assoc. Petrol. Geol. Mem., Tulsa, Okl., 1995.
- Engdahl, E., R. Van der Hilst, and R. Buland, Global teleseismic earthquake relocation with improved travel times and procedures for depth determination, *Bull. Seismol. Soc. Amer.*, *88*, 722–743, 1998.
- Gephart, J., Topography and subduction geometry in the central Andes: Clues to the mechanics of a noncollisional orogen, *J. Geophys. Res.*, *99*, 12,279–12,288, 1994.
- Gubbels, T., B. Isacks, and E. Farrar, High-level surfaces, plateau uplift, and foreland development, Bolivian Central Andes, *Geology*, *21*, 695–698, 1993.
- Isacks, B., Uplift of the central Andean plateau and bending of the Bolivian orocline, *J. Geophys. Res.*, *93*, 3211–3231, 1988.
- Jeyakumar, M., J. Rudnicki, and L. Keer, Modeling slip zones with triangular dislocation elements, *Bull. Seismol. Soc. Am.*, *82*, 2153–2169, 1992.
- Jordan, T., B. Isacks, R. Allmendigner, J. Brewer, V. Ramos, and C. Ando, Andean tectonics related to geometry of the subducted Nazca plate, *Geol. Soc. Am. Bull.*, *94*, 341–361, 1983.
- Kanamori, K., Rupture process of subduction zone earthquakes, *Ann. Rev. Earth Planet. Sci.*, *14*, 187–198, 1986.
- Kendrick, E., M. Bevis, R. Smalley, O. Cifuentes, and F. Galban, Current rates of convergence across the Central Andes: Estimates from continuous GPS observations, *Geophys. Res. Lett.*, *26*, 541–544, 1999.
- Kendrick, E., M. Bevis, R. Smalley, and B. Brooks, An integrated crustal velocity field for the Central Andes, *Geochem. Geophys. Geosyst.*, *2*, 10.1029/2001GC000191, 2001. (Available at <http://g-cubed.org>)
- Kley, J., Der Übergang vom Subandin zur Ostkordillere in Südbolivien (21°15–22°S), Geologische, struktur und kinematik, Ph.D. dissertation, Freie Univ., 1993.
- Kley, J., Transition from basement-involved to thin-skinned thrusting in the Cordillera Oriental of southern Bolivia, *Tectonics*, *15*, 763–775, 1996.
- Kley, J., Geologic and geometric constraints on a kinematic model of the Bolivian orocline, *J. South Am. Earth Sci.*, *12*, 221–235, 1999.
- Kley, J., and C. Monaldi, Tectonic shortening and crustal thickening in the Central Andes: How good is the correlation?, *Geology*, *26*, 723–726, 1998.
- Klotz, J., J. Reinking, and D. Angermann, Die vermessung der deformation der erdoberflaeche, *Geowissenschaften*, *14*, 389–394, 1996.
- Klotz, J., D. Angermann, G. Michel, R. Porth, C. Reigber, J. Reinking, J. Viramonte, R. Perdomo, V. Rios, S. Barrientos, R. Barriga, and O. Cifuentes, GPS-derived deformation of the Central Andes including the 1995 Antofagasta $M_w = 8.0$ Earthquake, *Pure Appl. Geophys.*, *154*, 709–730, 1999.
- Lamb, S., Active deformation in the Bolivian Andes, South America, *J. Geophys. Res.*, *105*, 25,627–25,653, 2000.
- McCaffrey, R., Global variability in subduction thrust zone — Forearc systems, *Pure Appl. Geophys.*, *142*, 173–224, 1994.
- Mingramm, A., A. Russo, A. Pozzo, and L. Casau, Sierras subandinas, in *Segundo Simposio de Geología Regional Argentina*, pp. 95–138, Acad. Nacional de Ciencias, Córdoba, Argentina, 1979.
- Norabuena, E., L. Leffler-Griffin, A. Mao, T. Dixon, S. Stein, I. Sacks, L. Ocala, and M. Ellis, Space geodetic observation of Nazca — South America convergence across the Central Andes, *Science*, *279*, 358–362, 1998.
- Norabuena, E., T. Dixon, S. Stein, and C. G. A. Harrison, Decelerating Nazca — South America and Nazca — Pacific motions, *Geophys. Res. Lett.*, *26*, 3405–3408, 1999.
- Pardo-Casas, F., and P. Molnar, Relative motion of the Nazca (Farallon) and South American plates since Late Cretaceous time, *Tectonics*, *6*, 233–248, 1987.
- Peterson, E., and T. Seno, Factors affecting seismic moment release rates in subduction zones, *J. Geophys. Res.*, *89*, 10,233–10,248, 1984.
- Randall, D., A new Jurassic - Recent apparent polar wander path for South America and a review of central Andean tectonic models, *Tectonophysics*, *299*, 49–74, 1998.
- Roeder, D., and R. L. Chamberlain, Structural geology of Sub-Andean fold and thrust belt in northwestern Bolivia, in *Petroleum basins of South America*, 62, edited by A. J. Tankard, S. R. Suárez and H. J. Welsink, pp. 459–479, Am. Assoc. Petrol. Geol. Mem., Tulsa, Okl., 1995.
- Ruff, L., and K. Kanamori, Seismicity and the subduction process, *Phys. Earth Planet. Int.*, *23*, 240–252, 1980.
- Savage, J. C., A dislocation model of strain accumulation and release at a subduction zone, *J. Geophys. Res.*, *88*, 4984–4996, 1983.
- Scholz, C., The mechanics of earthquakes and faulting, 439 pp., Cambridge Univ. Press, New York, 1990.
- Somoza, R., Updated Nazca (Farallon) — South America relative motions during the last 40 My: Implications for mountain building in the central Andean region, *J. South Am. Earth Sci.*, *11*, 211–215, 1998.
- Uyeda, S., Subduction zones: An introduction to comparative subductology, *Tectonophysics*, *81*, 133–159, 1982.
- Wdowinski, S., R. O'Connell, and P. England, A continuum model of continental deformation above subduction zones: Application to the Andes and the Aegean, *J. Geophys. Res.*, *94*, 10,331–10,346, 1989.